Background

The figure at the right shows a typical set of images from Echo Planar Imaging (EPI) fMRI experiments (Ojemann, et al. 1997). These "slices" of a human brain in three different planes are produced using an experimental arrangement pictured in the diagram below.

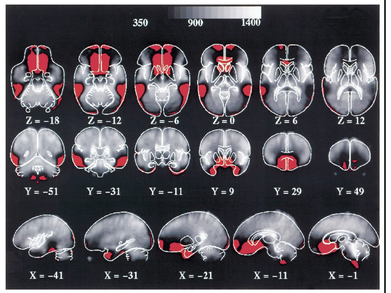

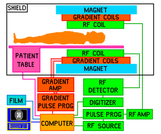

fMRI experimental arrangement
(from J. P. Hornak, The Basics of MRI © 1996 - 2013
http://www.cis.rit.edu/htbooks/mrihttp://www.cis.rit.edu/htbooks/mri)

The subject lies in a powerful static magnetic field that is provided by a superconducting magnet.
The field $\mathbf{B_0}$ is directed along the axis of the body and head (the **z**-axis), and may be as large as 3 T. The radio frequency (RF) coil and the gradient coils are contained within a headset worn by the subject that directs their fields along the same axis. The RF coil is responsible for generating the RF fields that change nuclear spin orientations in the magnetic field and for detecting the fields that are generated when the spins relax to their normal orientations. It is the gradient coils that enable the signal to be mapped to a planar "slice". This is done by producing additional time varying magnetic fields B_{grad} that, although also oriented along the **z**-axis, vary linearly in magnitude along the **x, y**, or **z** axis. It is these pulsed fields that produce the electrical (**E**) fields that are of concern in this study. The gradient fields are controlled by the Gradient Pulse Programmer, under control of the computer, in order to produce a complex set of interleaved pulses in B_{grad} such as those pictured in the figure from http://practicalfmri.blogspot.com/ shown below at the left.

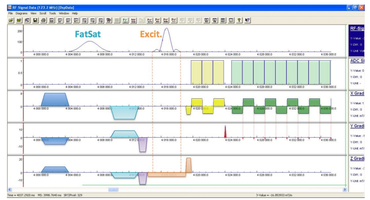

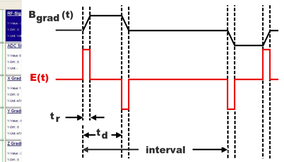

Faraday's law states that the time-varying B_{grad} fields along the **z**-axis will produce E fields in the **x-y** plane that are proportional to the rate of change of B_{grad} with time, dB_{grad}/dt. For these trapezoidal pulses, B_{grad} is constant except for the linear ramps up and down from a maximum value. During this rise time and fall time t_r, B_{grad} is changing at a constant rate, and a constant E field is induced in the brain. This is illustrated in the figure to the right above. Here a positive B_{grad} pulse has rise and fall times t_r, and begins to fall after a delay t_d. As a result, it produces a positive E field pulse of width t_r, followed by a negative one at a time t_d later. In this example, the B_{grad} pulse that follows after a time 'interval' is a negative one. This produces pairs of E field pulses with the negative pulse preceding the positive one.

Some differences between pyramidal cell and axon models

At the relatively low switching frequencies used in fMRI (< 10 kHz) a quasi-static approximation holds. Then, electric fields that are transverse to the membrane surface, produce a nearly instantaneous shift in intracellular membrane potential Vm that is proportional to the field and the diameter of the cell or axon at that point. (Ye et al. 2011). This has different consequences for cortical pyramidal cells than for axons:

- Typical unmyelinated cortical intralaminar axon diameters are one or two micrometers, whereas the pyramidal cell dendrites and soma are much thicker. Peripheral nerve axons have diameters that are comparable to dendrites.
- Cortical geometry does not lend itself to the production of longitudinal E fields, because the long axes of the pyramidal cells of the auditory and visual cortices are oriented perpendicularly to the cortical surface, transverse to the induced electric fields.
- The fast sodium and delayed rectifier potassium channels in axons provide the function of reliably delivering APs, with minimal disruptions of their timing, unlike cortical neurons.

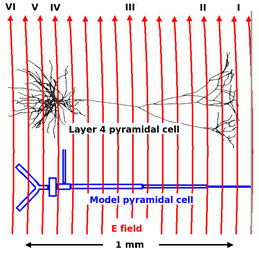

Pyramidal cells have additional calcium and calcium concentration dependent potassium channels with slower dynamics that prolong the hyperpolarized period following an AP. This contributes to spike frequency adaptation and causes a greater sensitivity to inputs that occur when the cell is near threshold for firing, enabling information to be encoded in spike timing. These characteristics are responsible for the different sensitivity of the axon and pyramidal cell models to perturbations and the effect of t_r and t_d.

Our approach

Used an existing GENESIS (Bower and Beeman 1998) model of the thalamorecipient layer of primary auditory cortex (Beeman 2013). The ACnet2 model provides sufficient biological realism to predict behavior, yet is simple enough for analysis. The customizable model provides:

- o Network of 2304 pyramidal cells and 576 inhibitory basket cells
- o 9-compartment pyramidal cells representing a simplified yet accurate neocortical pyramidal morphology
- o Synaptic and voltage activated conductances fit to experiment
- o Synaptic inputs at appropriate dendritic locations
- o Decay of connection probability with distance, fit to experiment
- o Input from other cortical areas was represented by a Poisson-distributed random spike train with a mean frequency of 8 Hz.

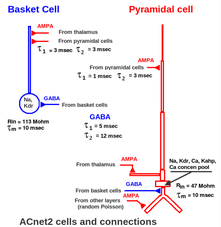

ACnet2 cells and connections

In the original simulations, the excitatory postsynaptic current (EPSC) arising from connections between the pyramidal cells was used to visualize and analyze the propagation and interaction of cortical waves. The total summed EPSC over ***all*** pyramidal cells has these characteristics:

- It is a sensitive measure of cortical activity that is difficult to discern from spike train analysis of APs
- It is proportional to the signal measured in MEG experiments
- Its Power Spectral Density (PSD) obtained by Fourier transform can reveal responses to periodic stimulation

In the 'fMRInet' version of the model, typical fMRI-generated E fields were applied to the network, while it was undergoing normal background activity in the absence of auditory stimulation.

E fields were calculated for trapezoidal B pulses with durations t_d and rise times t_r typical of those used in echo planar imaging (EPI) fMRI.

Both longitudinal (1) and transverse (2) E field models were implemented, with an emphasis on (2), which had a larger effect in the simulations.

Results

It is very difficult to discern an effect on cell firing from the plots of cell Vm above, even when zooming in, as in the insert. The synaptic currents (e.g. EPSCs) arising from connections are a very sensitive measure of network activity, but the plots at the right in the figure above are hard to decipher. The GENESIS 'replay_netview' tool performs a post-run analysis from data files that were generated and marked with a "RUNID". In addition to recreating the Vm plots, and presenting a visualization of network activity, it calculates the average firing frequency of the pyramidal and basket cells, and a power spectral density of the summed EPSCs.

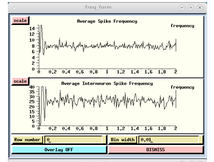

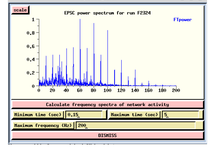

The screen image to the right shows that the effect on firing is noticeable, but small, in the plot of average spike frequency. However, the power spectrum of the summed EPSCs shows very strong effects at 10 Hz intervals, corresponding to the perturbation every 0.1 sec.

In order to determine the threshold E field for a "noticeable effect" in the PSD, we looked for perturbations at 100 Hz that were of approximately the same level as the normal spectrum between 20 and 40 Hz.

This is illustrated in the plot that compares the PSD for a standard single pulse sequence at E field values of 50, 40, 30, and 20 V/m with that when no fMRI pulse is present. From this, we estimated the threshold E_{thresh} to be 40 V/m for transverse E fields. Note that the transition was sharp enough to estimate the threshold with about 20% precision.

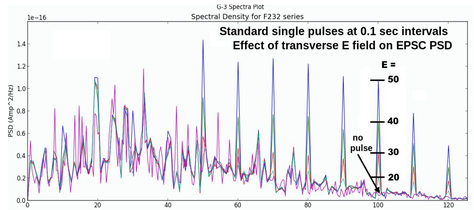

When similar inputs are applied, but with a negative B pulse, the the negative E pulse precedes the positive one, and the cells are inhibited first, and then excited. A plot of the PSD for different E field magnitudes, similar to the one above for positive pulses, indicates that this produces a slightly less effect, with E_{thresh} = 70 V/m.

Effect of positive and negative E pulse delay

The figure shows the EPSC PSD plots obtained from simulated effects of transverse E fields on the fMRInet model undergoing normal background activity in the absence of auditory stimuli (blue), and with additional simulated fMRI pulses applied every 12.5 msec, t_r = 0.2 msec, t_d = 1 msec (red), and t_d = 5 msec (green), illustrating the effect of increasing t_d. An above-threshold value of E = 70 V/m was used. This, and runs with shorter and longer t_d illustrate that there will be maximum effect if the "window" of time between the depolarizing and hyperpolarizing pulses brackets the span the width of an action potential.

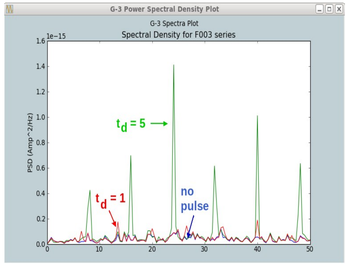

Conclusions and recommendations

As expected, the simulated fMRI-induced currents did not directly fire APs in the model neurons when they were quiescent. However, when the cells were in an active (AP firing) state the pattern of activity could be appreciably modified by such induced currents. Thus it seems likely that ongoing activity in neocortical neural networks would be perturbed (modulated) by the imposition of an fMRI field.

Even though such modulations may not evidence themselves as directly evoked sensory responses to fMRI, they could quite likely modify the response of the brain to other stimuli (flashes of light,sounds words etc.) As such, they represent a source of artifacts in localizing the brain's response to the sort of stimuli typically presented during fMRI based studies. For example, locating the locus of word associations in the cortex (as in a "Stroop test") could be adversely affected by the confounding effects of fMRI induced currents. Short term exposures to fMRI fields might produce some minor changes in ion concentrations,synaptic transmitter release etc but are unlikely to cause long lasting effects. However, prolonged and repeated exposures to the currents such fields induce may result in adverse "plastic" effects. For example, recent studies (such as those of concussion injury in football players) point to the possibility that the cumulative neural effect of repeated, seemingly innocuous, perturbations can be substantial.

Some recommendations for follow up study, beyond those listed under **Future work,** include:

1. The implications of these simulation studies need to be tested in living animals wherein cortical signal processing can be monitored before, after and (hopefully) during the imposition of intracranial currents similar to those induced by fMRI fields.

2. If the experimental results substantiate the model's implications, the casual use of fMRI in studies of human volunteers should be discouraged (or banned).

3. If a human study using fMRI is deemed to be especially cogent and important the "volunteer" subjects must be properly informed of the risks and benefits involved and be able to make informed judgments as to their participation.

4. Part of this "informed consent process" should include the opportunity to do long term follow up tracking of subjects to determine what, if any, neural deficits arise over time. To the extent possible this should also retrospectively examine consequences of earlier fMRI exposure -- especially in "volunteers" that had been in prolonged or multiple studies.

Acknowledgment: David Beeman was partially supported by NIH grant R01 NS049288-06 to James M. Bower.

Obtaining the simulation scripts: The full description of the ACnet2 network model, simulation scripts, and tutorial documentation may be downloaded from http://genesis-sim.org/ACnet2. The simulation scripts for the fMRInet variation used in this study will be available in December from http://genesis-sim.org/GENESIS/fMRInet.

References

Beeman D (2013) A modeling study of cortical waves in primary auditory cortex. BMC Neuroscience, 14(Suppl 1):P23 doi:10.1186/1471-2202-14-S1-P23

Bower JM, Beeman D (1998, 2003) The Book of GENESIS: Exploring Realistic Neural Models with the General NEural SImulation System, second edn. Springer-Verlag, New York. Free internet edition available at: http://www.genesis-sim.org/GENESIS/iBoG/iBoGpdf

Ojemann JG, Akbudak E, Snyder AZ, McKinstry RC, Raichle ME, Conturo TE (1997) Anatomic Localization and Quantitative Analysis of Gradient Refocused Echo-Planar fMRI Susceptibility Artifacts. Neuroimage 6:156-167.

Reilly JP (1989) Peripheral nerve stimulation by induced currents: exposure to time-varying magnetic fields. Med & Biol Eng and Comput 27:101-110

Roth BJ, Basser PJ(1990) A model of the stimulation of a nerve fiber by electromagnetic induction. IEEE Trans Biomed Eng 37:588 - 597

Ye H, Cotic M, Fehlings MG, Carlen PL (2011) Transmembrane potential generated by a magnetically induced transverse electric field in a cylindrical axonal model. Med Biol Eng Comput (2011) 49:107–119 DOI 10.1007/s11517-010-0704-0